Prepublished Copy

NATURE ENVIRONMENT AND POLLUTION TECHNOLOGY

Article In Press

PEER-REVIEWED PREPUBLISHED MANUSCRIPT

This is a peer-reviewed prepublished version of the paper to be published in **Vol. 26, No. 1, March 2027.**

Pilot-Scale Treatment of Sunfix Red SPD Dye Wastewater Using MBBR-UV Fenton: Optimization Using BBD-RSM With Economic Analysis

S. Prabhudesai and S. Mutnuri

RECEIVED
6 May 2026

CITE THIS ARTICLE

S. Prabhudesai and S. Mutnuri, 2027. Pilot-Scale Treatment of Sunfix Red SPD Dye Wastewater Using MBBR-UV Fenton: Optimization Using BBD-RSM With Economic Analysis. Nature Environment and Pollution Technology, 26(1), B4452.

https://doi.org/10.46488/NEPT.2027.v26i01.B4452

EARLY-ACCESS STATEMENT

This manuscript, after peer review, is being released online in its original, unedited form to provide early access to its findings. Prior to final publication, it will undergo additional editing and formatting. Readers may note that, as an unedited version, the manuscript may have linguistic and other minor errors. The DOI will be active after the final publication of the paper.

PUBLICATION STATUS

PEER REVIEW	ONLINE VERSION	FINAL ISSUE
Completed	**Prepublished**	**March 2027**

Original Research

Pilot-Scale Treatment of Sunfix Red SPD Dye Wastewater Using MBBR-UV Fenton: Optimization Using BBD-RSM With Economic Analysis

S. Prabhudesai and S. Mutnuri†

Water, Sanitation and Hygiene Lab, Department of Biological Sciences, BITS-Pilani, K.K. Birla Goa Campus, Goa, 403726, India, p20200005@goa.bits-pilani.ac.in
†Corresponding author: Srikanth Mutnuri; srikanth@goa.bits-pilani.ac.in
ORCID IDs of Authors 0000-0003-3575-6812

Abstract

Dye contamination in wastewater is a serious environmental problem, especially in industries such as textiles, food, and pharmaceuticals. These dyes are complex in structure, high in molecular weight, water soluble, resistant to degradation, and known carcinogenic and mutagenic agents. Consequently, the development of effective technologies for dye degradation is imperative. This work has investigated the application of biological treatment, such as Moving bed biofilm reactor (MBBR), with chemical treatment, such as UV/Fenton's reaction, for effective degradation of Sunfix red spd dye (SR). The Box-Behnken statistical experimental design was used to optimize the degradation of SR dye. Furthermore, the integrated MBBR-UV/Fenton system showed very high removal efficiencies, decreasing color by > 98%, Chemical Oxygen Demand (COD) by 84-88%, Biological Oxygen Demand (BOD_5) by > 98%, and Ammoniacal nitrogen (NH_4-N) by 70-75%. Similar results were observed when the system was scaled up to 1000 L/d, wherein the system reduced color by 98.89%, COD by 94.97%, BOD_5 by 94.63%, and NH_4-N by 79.91%. Additionally, HPLC analysis validated the disappearance of the parent compound, confirming dye degradation using the MBBR-UV/Fenton system. Thus, the combination of both MBBR and UV/Fenton process showcases a highly effective and promising solution for dye wastewater treatment.

Keywords
Dye degradation, UV-Fenton reaction, Moving Bed Biofilm Reactor, HPLC dye degradation

Graphical Abstract

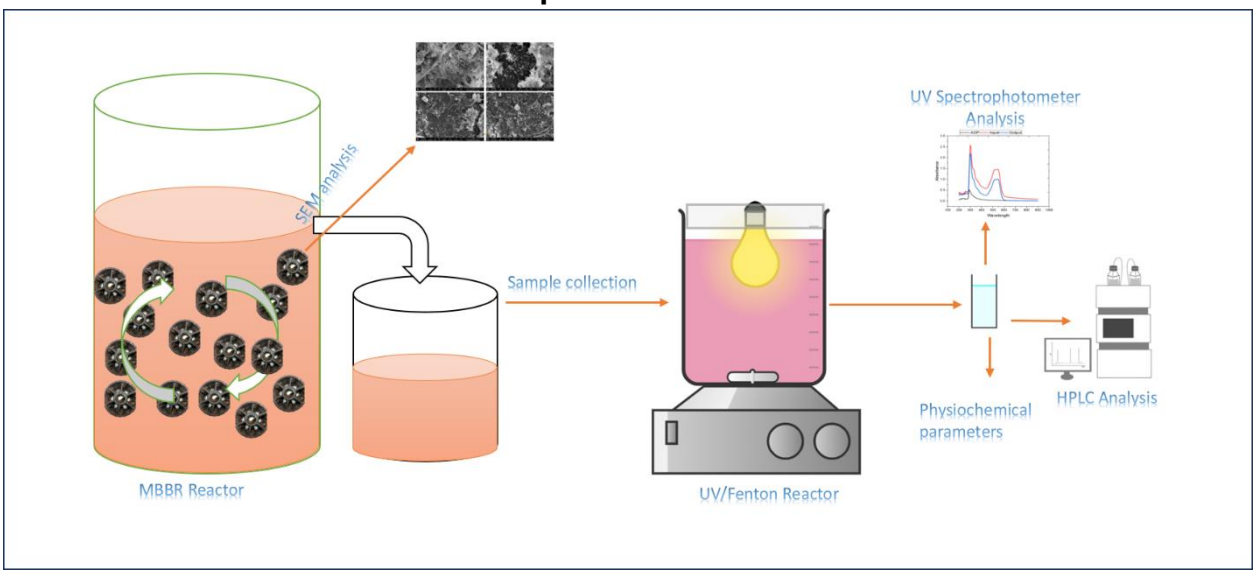

1. INTRODUCTION

The increasing contamination of water resources has emerged as a critical environmental challenge that requires effective and sustainable solutions. Among various industrial pollutants, dye-containing wastewater released from industries such as food processing, leather tanning, and textile manufacturing represents a major contributor to aquatic pollution. Industrial dyes are highly complex organic molecules characterized by high molecular weight, water solubility, structural stability, and resistance to natural degradation processes. Many of these synthetic dyes are reported to possess carcinogenic and mutagenic properties, posing significant risks to both environmental and human health. Furthermore, the intense coloration of dye effluents reduces light penetration into aquatic systems, thereby disrupting photosynthetic activity and negatively affecting aquatic ecosystems (Afanga et al. 2020; Kallawar and Bhanvase 2024).

To address this growing concern, extensive research efforts have been directed toward developing efficient, economical, and environmentally sustainable wastewater treatment approaches. Conventional treatment methods, including membrane filtration, coagulation, and chemical oxidation processes, often exhibit limitations in achieving complete dye degradation. Additionally, these approaches may generate toxic intermediates and secondary pollutants, further complicating wastewater management (Park et al. 2010; Kallawar and Bhanvase 2024). Therefore, there is a growing need to explore advanced treatment strategies that can overcome these limitations. Hybrid approaches integrating biological processes with chemical oxidation systems have gained attention due to their potential to enhance pollutant removal efficiency while minimizing environmental impacts. Such integrated systems offer promising opportunities for the effective treatment and sustainable management of dye-contaminated wastewater.

To overcome this limitation, the Moving Bed Biofilm Reactor (MBBR) can be combined with AOP for the biodetoxification of dyes. MBBR is a highly advanced biological wastewater treatment method that efficiently integrates suspended and attached growth systems (Gzar, Al-Rekabi, and Shuhaieb 2021, Yang and López-Grimau 2021). The major benefits of MBBR technology over conventional systems include a lower footprint, a higher concentration of biomass on the biocarrier, and resistance to shock organic loads (Francis and Sosamony 2016). Previous studies have consistently demonstrated superior performance of MBBRs, with a laboratory-scale MBBR achieving 86% COD removal and 81.5% BOD removal within 2.25 days at optimal conditions (Francis and Sosamony 2016). Hybrid Moving Bed Biofilm Reactor-Membrane Bioreactor (MBBR-MBR) systems have reported 93% COD removal, 85% color removal, and 99% total suspended solids (TSS) removal with a hydraulic retention time of merely one day (Yang and López-Grimau 2021). Economically, MBBR is a more appealing option than MBR because of lower construction costs (CAPEX) and equivalent operational costs (OPEX), resulting in lower effluent discharge taxes and water cost savings. Furthermore, MBBR systems demonstrate fewer environmental consequences across multiple categories, particularly in climate change, due to the reduction in the need for triamine-based decolorizing chemical substances (Yang and López-Grimau 2021).

Advanced Oxidation Processes (AOPs) are known as very successful procedures for cleaning water and wastewater containing hazardous and non-biodegradable contaminants. They achieve high reaction yields and offer cost-effective sources of potent oxidizing agents (Lucas and Peres 2006, PIECZYKOLAN, PŁONKA, and BARBUSIŃSKI 2016). The Fenton and UV/Fenton reactions are very promising (Papić *et al.* 2009). The Fenton process produces extremely reactive hydroxyl radicals (·OH) by reacting hydrogen peroxide (H_2O_2) with ferrous iron (Fe^{2+}) in an acidic environment (Papić *et al.* 2009, Tuncer and Sönmez 2023). These hydroxyl radicals are effective, non-selective oxidizers that can break down complex organic contaminants, like dyes, to smaller molecules, often causing them to mineralize into CO_2 and H_2O (Papić *et al.* 2009, Phanwilai *et al.* 2020). The Fenton reaction produces high yields in the acidic pH range from 2 to 3, but one main disadvantage of the reaction is the generation of ferric hydroxide sludge, which requires additional treatment and disposal (Phanwilai *et al.* 2020, Gzar Al-Rekabi and Shuhaieb 2021, Kallawar and Bhanvase 2024).

Integrating UV light in the conventional Fenton reaction significantly increases the photo-reduction of ferric (Fe^{3+}) ions to ferrous (Fe^{2+}) ions, renewing the catalyst and generating ·OH radicals (Papić *et al.* 2009, Phanwilai *et al.* 2020). This leads to an increase in mineralization and decolorization efficiency of textile wastewater compared to the Fenton reaction alone. Studies have shown that the homogeneous UV/Fenton process (UV/Fe^{2+}/H_2O_2) is highly effective, achieving high levels of decolorization (95–100%)

and mineralization (78–84%) of reactive dyes (Papić *et al.* 2009). Furthermore, the UV/H_2O_2 process (without added iron) is considered an environmentally friendly alternative to Fenton, as it generally produces less sludge (Nagel-Hassemer *et al.* 2011).

The objective of the present study is to investigate a pilot-scale treatment system (1000L/d) for the degradation of Sunfix Red SPD (SR) dye, using a biological pre-treatment, such as MBBR, and further integrating it with advanced oxidation processes in a series, such as a UV/Fenton system, and to use Box-Behnken design to optimize parameters for maximum degradation efficiency. The parameters were pH, Time, and concentration. of H_2O_2 and conc. of $FeSO_4$. The high-performance liquid chromatography (HPLC) was utilized to monitor the mineralization of the parent dye.

2. MATERIALS AND METHODS

2.1. PREPARATION OF SYNTHETIC DYE SPIKED MUNICIPAL WASTEWATER

SR dyes were procured locally and subsequently dissolved in municipal wastewater to prepare dye wastewater at a concentration of 100 ppm. This wastewater was used to evaluate the effectiveness of treatment processes for dye removal.

2.2. LAB-SCALE MBBR REACTOR

A laboratory-scale MBBR was constructed using a cylindrical plastic bucket with a height of 20 cm and a diameter of 30 cm, providing an effective working volume for the experimental setup. Polypropylene carriers, which have a specific surface area of 500 m^2/m^3, were introduced into the reactor to serve as biocarriers, facilitating biofilm development and microbial attachment. The carriers were added at a filling ratio of 50% of the total reactor volume. Two peristaltic pumps (NFP-01, Flow-tech) were connected to the MBBR reactor, which provided a constant flow rate of influent at 7 mL/min. In addition, a round epidium bubble diffuser was placed at the bottom, which was connected to two air blowers (Hailea HAP, Amazon), which ensured uniform carrier circulation and mixing. The MBBR was inoculated with activated sludge freshly collected from BITS Pilani, Goa campus sewage treatment plant.

2.3. LAB-SCALE UV/FENTON REACTION SETUP

A batch UV-Fenton reactor was constructed using a 2 L glass beaker as the reaction vessel. An immersible UV lamp 9W (Arhaan Enterprises) was suspended inside the beaker. To prevent the escape of UV light, the beaker was wrapped with aluminum foil. A magnetic bead was placed inside the beaker, and the assembly was kept on a magnetic stirrer (IKA C-MAG HS7 digital, Merck) to maintain continuous agitation during the reaction. For each experiment, 2 L of dye wastewater previously treated by the MBBR reactor was collected and transferred into the beaker. The pH of the wastewater was adjusted using 1M Sulfuric acid (H_2SO_4) and 1M Sodium Hydroxide (NaOH). After which, an optimized amount of H_2O_2 and $FeSO_4.7H_2O$ (LOBA) was added into the beaker and stirred for a specific interval in the presence of UV light (Nagel-Hassemer *et al.* 2011).

2.4. SCANNING ELECTRON MICROSCOPY.

Biofilm morphology was characterized at high resolution using SEM analysis. A small part of the biocarrier was treated with 4% glutaraldehyde for an entire night at 4°C. To get rid of any remaining fixative, the fixed sample was washed three times with phosphate-buffered saline (PBS). Furthermore, sequential dehydration was carried out using ethanol gradients (30%, 50%, 70%, 90%, and 100% v/v). To improve conductivity, a 10 nm coating of palladium-gold alloy was applied to dehydrated specimens using a LEICA EM ACE 200 sputter coater. A field-emission scanning electron microscope (FEI QUANTA FEG 250, Netherlands) operating at an accelerating voltage of 5–10 kV under high vacuum conditions was used for imaging.

2.5. EXPERIMENTAL DESIGN USING BBD - RSM

To optimize the UV-Fenton reaction, a BBD-RSM was used with four factors, and a three-level Box-Behnken design (BBD) was constructed. The factors were Time (20-60 min), pH (2-10), H_2O_2 conc. (20-100 mg/l) and $FeSO_4$ conc. (20-100 mg/l), based on preliminary screening experiments. The design generated 29 experimental runs, including replicated center points, which were carried out at constant initial COD and temperature. The experimental data were fitted to a second-order polynomial of the form.

$$Y=\beta_0+\sum\beta_i X_i+\sum\beta_{ii} X_i^2+\sum\beta_{ij} X_i X_j \quad (1)$$

where Y is the predicted response (COD or color removal), X_i are the coded independent variables, and β are the regression coefficients. Model fitting, analysis of variance (ANOVA), and generation of 3D response surfaces and contour plots were performed using Design Expert software (version 13), which was also used to identify the optimal operating conditions through numerical desirability analysis. The validation experiments for all optimized variables were carried out to assess the reproducibility of the results by evaluation of residual cod removal, degradation efficiencies at 299nm, and 543nm.

2.6. PHYSICO-CHEMICAL PARAMETERS

Samples were collected once every week post each treatment stage: dye wastewater (Input), MBBR output (MO), and post-UV/Fenton effluent (UV-Fenton), in 1L sampling bottles. All samples were analyzed within 24 hours of collection to minimize compositional changes. Each sample was then analyzed using a UV spectrophotometer (Spectroquant Prove 100, Merck) for absorbance. Chemical Oxygen Demand (COD) was measured using the 5220 D closed reflux colorimetric method, Biological Oxygen Demand (BOD_5) was determined after a 5-day incubation at 20°C, and pH was measured with an Oakton pH 510 Series Meter (P/N 54X002608). Total Organic Carbon (TOC), Total Carbon, and Total Nitrogen (TN) were analyzed using a Shimadzu TOC-TNM-L ROHS analyzer.

2.7. HPLC ANALYSIS

High-performance liquid chromatography (HPLC) analysis was performed using a Shimadzu LC-20AD system equipped with a Kromasil 100-5-C18 column (Cat No: M05CLA15; 4.6 mm inner diameter × 150 mm length; pore size: 100 Å; particle size: 5 µm). Before analysis, all samples were filtered through 0.22 µm membrane filters. Chromatographic separation was performed using a binary mobile phase consisting of acetonitrile (ACN) and Milli-Q (Indion LAB-Q Smart Type 2 10L) water mixed with 0.001% ammonium acetate. For SR dye, the flow rate was set at 0.8 mL/min with a total run time of 20 minutes, and detection was carried out at 299 nm and 543 nm. The injection volume for all analyses was 20 µL. Chromatographic data were acquired and processed using Shimadzu LabSolutions software. Different known concentrations of dye, such as 20 ppm, 40 ppm, 60 ppm, 80 ppm, and 100 ppm, were prepared in Milli-Q water (Indion Lab Q-smart water maker, India) by serial dilution. These standards were then processed through an HPLC machine, and the resulting chromatograms were recorded as the peak area of SR at their specific retention time. Using this data, a calibration curve was obtained of dye concentration vs mean area of the peak, and linear regression analysis was performed to determine the correlation coefficient (r^2) and assess method linearity.

2.8. PILOT-SCALE CONSTRUCTION AND OPERATION OF THE MBBR- UV/FENTON TREATMENT SYSTEM

A pilot-scale treatment system was constructed using a 1000 L intermediate bulk container (IBC), which was termed the MBBR reactor. The MBBR was filled to 50% of its working volume with polypropylene biofilm carriers. This tank was attached to two air blowers (Hailey HAP, Amazon) (120 L/min each), which were then connected to four 12-inch fine bubble diffusers installed at the bottom of the reactor. The continuous flow of 7L/min input was maintained using two peristaltic pumps (Flowtech, NFP 03), which operated alternatively for 24 hours. For the startup of the MBBR reactor, activated sludge from the SBR reactor was added, and the MBBR reactor was aerated for 48 hrs. MBBR effluent was then directed into a settling tank via gravity. Following the settling tank, the treated effluent was directed to a UV/Fenton reaction tank. Wherein, the pH of the water was adjusted to the desired acidic range (2- 3) using 1M H_2SO_4.

A 0.5 HP Kirloskar water pump was attached to this tank to continuously circulate the wastewater through a UV chamber, ensuring thorough mixing and exposure to UV irradiation during the Fenton reaction. After the reaction, the effluent water was neutralized to pH 6.5 – 7.5 using a 1M NaOH solution, and samples were collected once every seven days. The HRT of the MBBR- UV/Fenton system was 26 hours (MBBR HRT 24 hours, UV/Fenton tank 2 hours). The pilot scale system was operated for a duration of 60 days. The period of 30 days was provided for the acclimatization of the biofilm onto the carrier.

2.9. ECONOMIC ANALYSIS

The economic analysis of capital expenditures (CAPEX) and operational expenditures (OPEX) for the MBBR-UV/Fenton system is determined by considering individual cost contributions to the treating process.

3. RESULTS AND DISCUSSION

3.1. SCANNING ELECTRON MICROSCOPY ANALYSIS

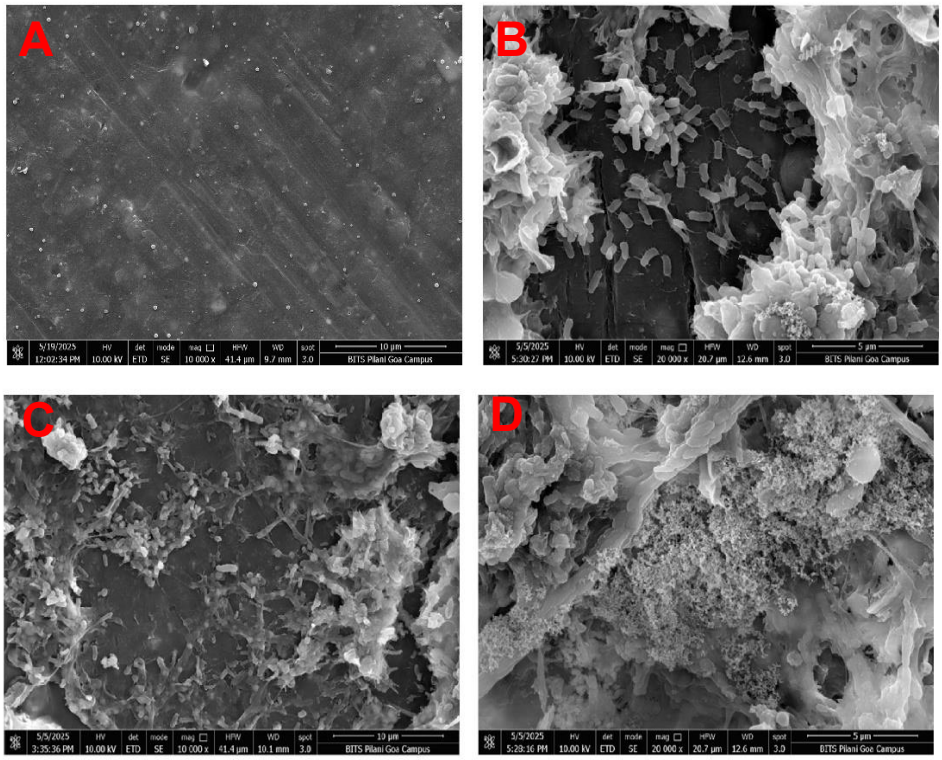

Fig. 1. SEM images of the biocarrier illustrating A) Control, B), C), and D) Rod-shaped morphology and a Cluster of different types of microbes.

The four SEM images depict the surface morphology and the microbial colonization of biofilm samples on the biocarrier used in the MBBR reactor. The images allow a detailed visualization of microbial structures and extracellular matrix on the carrier surface. Fig. 1 A shows the initial surface of the biocarrier at 10000 mag. It can be observed that the surface is very clean and free from biofilm, serving as a reference for comparison with post-experiment samples. Fig. 1 B, C, D shows a heterogeneous biofilm structure with multilayered bacterial growth attached to the internal surfaces and outer ridges of the plastic media, indicating extensive colonization on the bio-carrier. At higher magnifications, individual bacterial cells are more clearly resolved. It was observed that the carrier surface was predominantly colonized by rod- and coccus-shaped cells (Phanwilai *et al.* 2020). These findings also align with the author (Wang *et al.* 2023), confirming the development of biofilm structure essential for organic and nutrient removal.

3.2. STATISTICAL ANALYSIS AND MODELING VIA BBD-RSM.

The most significant parameters that affect the efficiency of SR decolorization in the UV/Fenton system are pH, Time, and the concentration of H_2O_2 and concentration of $FeSO_4$. To study the combined effects of these parameters, different statistically designed experiments were conducted, and the results of the response were recorded accordingly, as indicated in **Table 1**. The resulting experiment runs were confirmed for cubic, linear, quadratic, and two-factor interaction models.

This helped to identify a suitable model enabling the correlation in the UV/Fenton system of SR dye. The results for the Lack of fit tests have successfully pointed towards the quadratic form being best defined by the SR discoloration parameters (Table S1, Table S2, and Table S3). The recommended quadratic equation resulted in the best statistically significant model and did not have a significant lack of fit derived from the Fisher variance ratio and probability value compared to the cubic, linear, and the two-factor interaction models. The optimum values for the **COD removal efficiency** (R_1), **Degradation efficiencies at 299 nm** (R_2), and 543nm (R_3).

$$R_1 = 49.64 + 7.45*A - 17.64*B + 4.44*C + 3.23*D + 2.71*AB + 0.68*AC - 3.46*AD + 2.54*BC - 3.68*BD + 4.18*CD + 0.56*A^2 + 13.66*B^2 - 4*C^2 - 0.3961*D^2 \quad \textbf{(2)}$$

$$R_2 = 45.93 + 7.75A - 16.73*B + 3.95*C + 3.46*D - 0.4975*AB - 0.7*AC - 2.98*AD + 2.09*BC + 0.2225*BD + 6.37*CD + 0.486*A^2 + 15.98*B^2 - 5.22*C^2 - 2.57*D^2 \quad \textbf{(3)}$$

$$R_3 = 36.62 + 7.27*A - 19.48*B + 4.77*C + 4.51*D + 0.7825*AB - 0.0675*AC - 5.71*AD + 3.14*BC - 2.59*BD + 6.25*CD + 4.52*A^2 + 23.38*B^2 - 2.87*C^2 + 3.14*D^2 \quad \textbf{(4)}$$

Table 1: Box-Behnken design matrix along with Actual vs Predicted values.

Run	Factor 1 A: Time	Factor 2 B: pH	Factor 3 C: H_2O_2 concentration	Factor 3 C: $FeSO_4$ concentration	COD removal efficiency (%)		Degradation efficiency at 299 nm (%)		Degradation efficiency at 543 nm (%)	
					Actual	Predicted	Actual	Predicted	Actual	Predicted
1	20	6	60	100	42.57	49.04	41.37	42.53	42.13	47.23
2	40	10	60	100	46.85	44.81	45.45	46.28	42.87	45.58
3	40	6	100	20	38.57	42.28	30.91	32.26	28.87	30.92
4	40	10	20	60	31.71	34.68	28.96	33.92	30.06	29.74
5	60	6	20	60	45.57	48.53	49.11	45.7	37.91	40.84
6	40	6	20	20	40.71	41.76	35.14	37.12	28.26	33.87
7	40	6	60	60	50.28	49.64	39.99	45.93	30.44	36.62
8	60	6	60	100	54.86	57.02	50.95	52.07	48.57	50.35
9	40	10	100	60	49.57	48.64	47.5	46	46.06	45.57
10	60	6	60	20	62.28	57.49	50.42	51.13	58.73	52.76
11	40	10	60	20	47.57	45.71	43.83	38.93	41.5	41.75
12	20	10	60	60	33.86	36.05	38.46	38.41	36.63	36.98
13	40	6	60	60	46.28	49.64	36.76	45.93	33.93	36.62
14	40	2	60	100	85.26	87.45	73.46	79.31	86.55	89.73
15	20	2	60	60	78.43	76.76	74.36	70.88	77.57	77.52
16	20	6	60	20	36.14	35.66	28.91	29.66	29.44	26.79
17	40	6	20	100	45.57	39.85	35.45	31.28	34.99	30.39

18	40	6	100	100	60.14	57.09	56.72	51.92	60.6	52.43
19	40	2	100	60	80.15	78.85	78.37	75.28	78.81	78.26
20	60	10	60	60	56.71	56.38	52.25	52.91	55.6	53.1
21	20	6	100	60	45.14	42.51	33.74	38.09	35.34	35.84
22	40	6	60	60	48.35	49.64	46.91	45.93	38.26	36.62
23	20	6	20	60	38.86	34.99	31.53	28.8	29.4	26.16
24	**60**	**2**	**60**	**60**	**90.45**	**86.25**	**90.14**	**87.38**	**93.41**	**90.5**
25	40	2	20	60	72.43	75.04	68.2	71.57	75.37	74.99
26	40	6	60	60	51.14	49.64	52.42	45.93	48.16	36.62
27	60	6	100	60	54.57	58.77	48.52	52.2	43.58	50.25
28	40	6	60	60	52.14	49.64	53.56	45.93	32.32	36.62
29	40	2	60	20	71.28	73.65	72.73	72.84	74.82	75.54

In equations (2), (3), and (4), the positive coefficient of a factor suggests that the response improves as the factor level increases, while a negative coefficient indicates a decline in response. The effect of each process variable together with its interactions, as shown in equations (2),(3) and (4), was evaluated by ANOVA present in Table S4, Table S5, and Table S6.

In the case of COD removal (%) (Table S4), it can be observed that A, B, C, D, B^2, and C^2 were significant terms, while for **degradation efficiency at 299 nm** (%), the terms A, B, D, CD, A^2, B^2, and D^2 were found to be significant. Furthermore, for **degradation efficiency at** 543 nm (%), it was seen that A, B, C, D, A^2, and B^2 were significant terms. Moreover, Table S4, Table S5, and Table S6 clearly show that the corresponding F values for COD removal, **degradation efficiency at 299 nm**, and 543 nm were 25.25, 15.31, and 20.25, respectively, along with a very low probability value (p-value <0.0001). Hence, the F values for stated response factors confirm their robust statistical significance and are adequate for process optimization.

The R^2 values for COD removal, **degradation efficiency at 299 nm**, and 543 nm were 0.9619, 0.9387, and 0.9529. Moreover, the values of predicted R^2 for the responses were 0.7941, 0.7733, and 0.8090, respectively. In addition, the predicted R^2 values were in reasonable agreement with the adjusted R^2 values (0.9238, 0.8774, and 0.9059), that is, the difference is less than 0.2. Hence, the models were adequate. Moreover, Fig. 2 demonstrates excellent agreement between the predicted and experimental values for COD removal, **degradation efficiency at 299 nm**, and 543 nm, showcasing the reliability of the model by predicted and adjusted R^2 values. The values of adequate precision for stated response factors were 17.07, 14.38, and 15.07, respectively. Moreover, values C.V.% that are 8%, 11.43%, and 12.29% indicate that the experiments were accurate and reliable.

Fig. 2. Predicted vs Actual graph for A) COD removal (%), B) D**egradation efficiency at 299 nm**, and C) D**egradation**

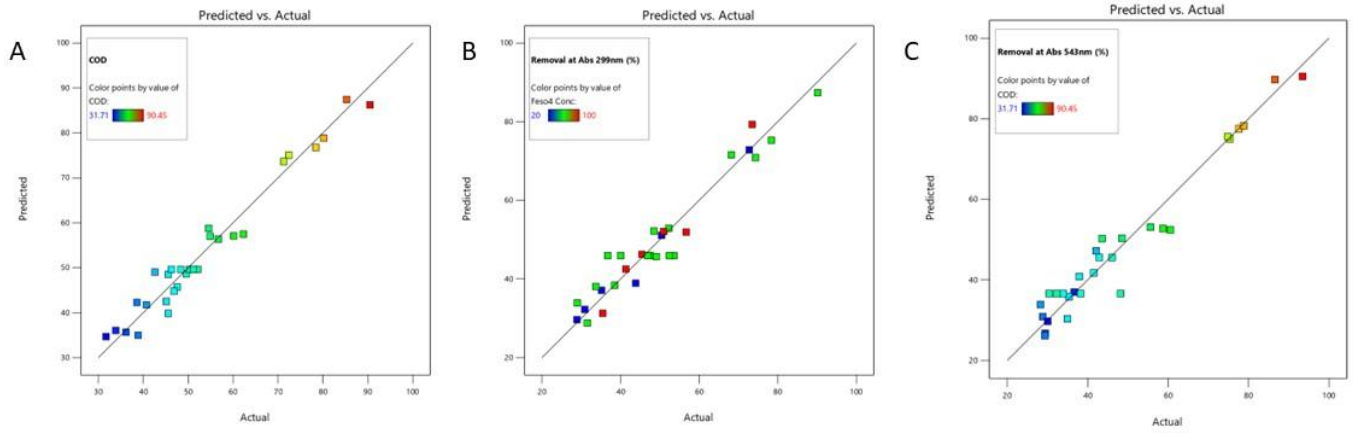

efficiency at 543 nm.

The maximum degradation efficiency was achieved during the 24th run (Table 1) at pH 2, Time 60 min, conc. of H_2O_2 and $FeSO_4$ was 60 mg/L each. Under these conditions, the highest efficiency of the treatment was achieved, indicating efficient degradation performance. Further, the validation experiments were performed to confirm the reliability and reproducibility of these optimized conditions. The validation experiment under optimum conditions yielded a COD removal efficiency of 84.18%, and the degradation efficiencies obtained by spectrophotometric analysis were 85.45% at 299 nm and 92.50% at 543 nm, respectively.

3.3. MUTUAL INTERACTION BETWEEN PARAMETERS.

The simultaneous effect of initial pH and reaction time is fundamental to the efficiency of Fenton-like processes, as these parameters collectively dictate the rate of the hydroxyl radical (OH) generation and the physical state of the iron catalyst (Agustina *et al.* 2019). Fig. 3A, 3D, and 3G depict the pH and time effect on COD removal, **degradation efficiency at 299 nm**, and 543 nm. While the concentration of H_2O_2 and $FeSO_4$ was kept constant. The optimal pH for activating H_2O_2 is between 2 and 3.5 (Haddad *et al.* 2014, Agustina *et al.* 2019). At this pH, iron species exist in their most active forms (such as hydrated ferrous ions or $Fe(OH)_2^+$ complexes), which efficiently decompose H_2O_2 into reactive radicals (Agustina *et al.* 2019). When pH is too low (pH < 2), efficiency decreases due to high concentration. of hydrogen ions that act as scavengers for hydroxyl radicals, forming water and reducing the amount of oxidant available for dye degradation (Haddad *et al.* 2014). The SR dye degradation was observed to decrease upon an increase in pH (> 4) as the solution becomes more alkaline, Fe^{3+} ions begin to precipitate as ferric hydroxides ($Fe(OH)_3$), leading to catalyst deactivation and formation of iron sludge (Agustina *et al.* 2019). Additionally, H_2O_2 becomes unstable and decomposes into oxygen and water rather than producing ·OH radicals (Tabaraki *et al.* 2023). This trend can also be observed in Fig. 3B, 3E, and 3H, indicating optimum pH and concentration of H_2O_2, which achieved maximum COD removal **and dye degradation**. Fig. 3A, 3D, and 3G also illustrate the trend of increasing COD removal and degradation efficiency at both wavelengths (299nm and 543nm). The SR dye showed faster degradation at the initial rapid phase, followed by a slower degradation, which might be attributed to the saturation of active sites on the catalyst surface with dye molecules (Chandrika *et al.* 2022). The Fig 3C, 3F, and 3I illustrate the effect of concentration of H_2O_2 and concentration of $FeSO_4$. The COD removal and degradation efficiency at both wavelengths (299nm and 543nm) was observed to be highest at a ratio of 1:1.

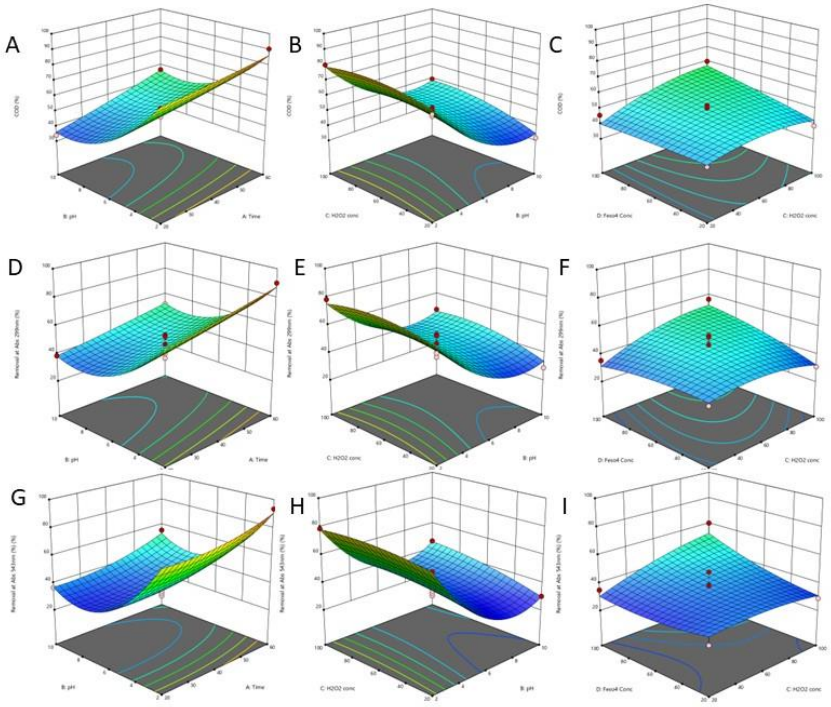

Fig. 3. Illustrates 3D contour plot of interactive effect A) pH vs Time B) concentration H_2O_2 vs pH C) concentration of $FeSO_4$ vs H_2O_2 for COD removal (%), D) pH vs Time, E) concentration H_2O_2 vs pH, F) concentration of $FeSO_4$ vs H_2O_2 for Degradation efficiency at 299 nm (%), and effect of G) pH vs time, H) concentration of H_2O_2 vs pH I) concentration of $FeSO_4$ vs H_2O_2 for Degradation efficiency at 543 nm (%) for SR dye.

3.4. PHYSICOCHEMICAL PARAMETERS

3.4.1. RESULTS OF COD AND BOD_5.

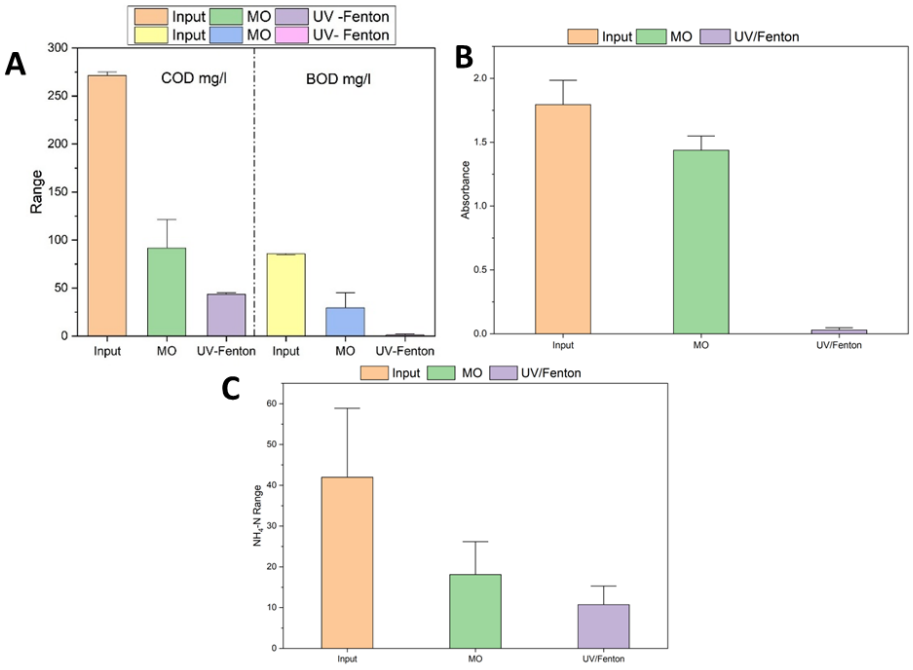

Fig. 4. Graph depicting average values of parameters after each treatment stage for SR dye A) COD and BOD_5, B) Change in absorbance at 543nm, C) Change in NH_4-N.

Fig. 4A shows average COD and BOD_5 values through different treatment stages present for SR dye. The influent (Input) COD concentration was 275 ± 64.71 mg/L. After MBBR output (MO), COD decreased to 91.75 ± 19.34 mg/l. Post which UV/Fenton treatment was conducted, which further reduced the COD to 43.5 ± 8.34 mg/l. The overall efficiency of the system for the reduction of COD was 84.18%. A similar trend was observed for BOD_5, Fig. 4A, the influent concentration was 85.8 ± 18.56 mg/l, which decreased to approximately 29.4 ± 8.54 mg/L after MBBR treatment and is nearly undetectable following UV/Fenton reaction, that is 1.14 ± 0.66 mg/l. Showcasing an efficiency of 98.6%. The error bars indicate that the UV-Fenton stage demonstrated lower variability in removal efficiency compared to the MBBR stage. The removal efficiencies demonstrated by MBBR of COD and BOD_5 for SR dye by 66 %. This reduction highlights the biofilm-assisted degradation of organic dye, confirming that MBBR plays a crucial role in the initial biodegradation of complex dye molecules (Samawi, Taba, and Lanuru 2025). However, the partial reduction also indicates the persistence of recalcitrant organic compounds that are not fully mineralized by biological treatment alone. The subsequent UV/Fenton reaction demonstrates the complementary role of the Fenton process in degrading residual dye molecules and refractory organics that withstand biological treatment, achieving COD removal for SR was 84.18%. For BOD_5, the system showed an efficiency of 98.6% for SR. Such near-complete elimination of biodegradable organic matter reflects the strong oxidative potential of the UV–Fenton process in mineralizing residual pollutants (Hu *et al.* 2011).

3.4.2. COLOR REMOVAL

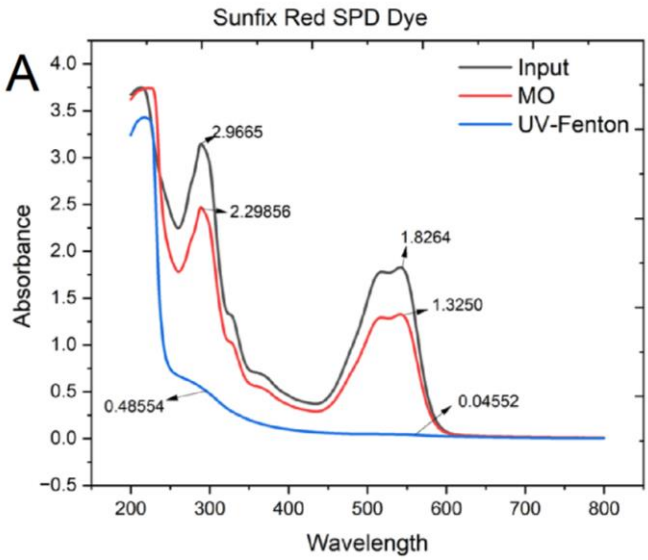

Fig. 5 A) Graph illustrating change in UV-visible spectrum for Input, MO, UV/Fenton of SR dye from 200-800nm.

From Fig. 4B, the initial absorbance of the SR dye was 1.794 ± 0.17, and after treatment in the MBBR, the absorbance was reduced to 1.43 ± 0.09, indicating a partial removal of the dye through the biological process. However, it was after the UV-Fenton stage that the complete decolorization and removal of the dye was achieved, showing an absorbance of 0.029 ± 0.016. The Overall system was very effective in the reduction of color, showing an efficiency of 98.37%. Fig. 5 A) shows the scan of the SR dye molecule over the spectrum ranging from 200nm to 800nm for Input, MO, and UV-Fenton, wherein degradation efficiency was 83.44% at 299 nm and 97.80% at 543 nm. The error bars were more pronounced in the Input and MBBR, indicating a greater variability in dye concentration at these points, while the UV-Fenton stage demonstrates consistent and reliable performance. The color removal by the UV-Fenton process, by generating highly reactive hydroxyl radicals through the Fenton reaction, significantly enhanced UV radiation. UV light promotes direct photolysis of H_2O_2 into hydroxyl radical and generates Fe^{2+} from Fe^{3+}, sustaining radical production. These non-selective hydroxyl radicals attack and break down the chromophoric groups of azo dye molecules, leading to decolorization of the dye molecules. These results align with the author Papić et al. (Papić *et al.* 2009), wherein the author investigated decolorization of three commercial reactive dyes by UV/Fe^{2+}/H_2O_2, achieving 95-10% color removal.

3.4.3. NH_4-N ANALYSIS

Ammonia nitrogen (NH_4-N) removal in the integrated MBBR–UV/Fenton system for dye wastewater was primarily attributed to the biological process, with advanced oxidation providing only minor additional removal. For SR, the influent NH_4-N concentration (41.98 ± 15.11 mg/L) was reduced to 18.1 ± 7.22 mg/L after MBBR treatment and further to 10.72 ± 4.07 mg/L following UV-Fenton, resulting in a total removal efficiency of 74.46% (Fig. 4C).

These findings are consistent with literature indicating that MBBR systems typically achieve 50–85% ammonia removal, leveraging biofilm-supported nitrification as the dominant removal pathway(Rusten *et al.* 2006, Chandrika *et al.* 2022, Samawi, Taba, and Lanuru 2025). The additional reduction by UV/Fenton is limited, in agreement with studies showing that Fenton and related advanced oxidation processes are far less effective for ammoniacal nitrogen than for organic pollutants, due to slow reaction kinetics and strong scavenging of reactive radicals by organic matter. Khatri et al. (Khatri *et al.* 2018) reported a maximum ammoniacal nitrogen removal of only 58.3% using zero-valent aluminum-based AOPs for textile wastewater. These findings consistently demonstrate that advanced oxidation processes prioritize organic pollutant degradation over nitrogen species oxidation in dye effluent matrices.

3.5. QUALITATIVE HPLC ANALYSIS OF THE SR DYE

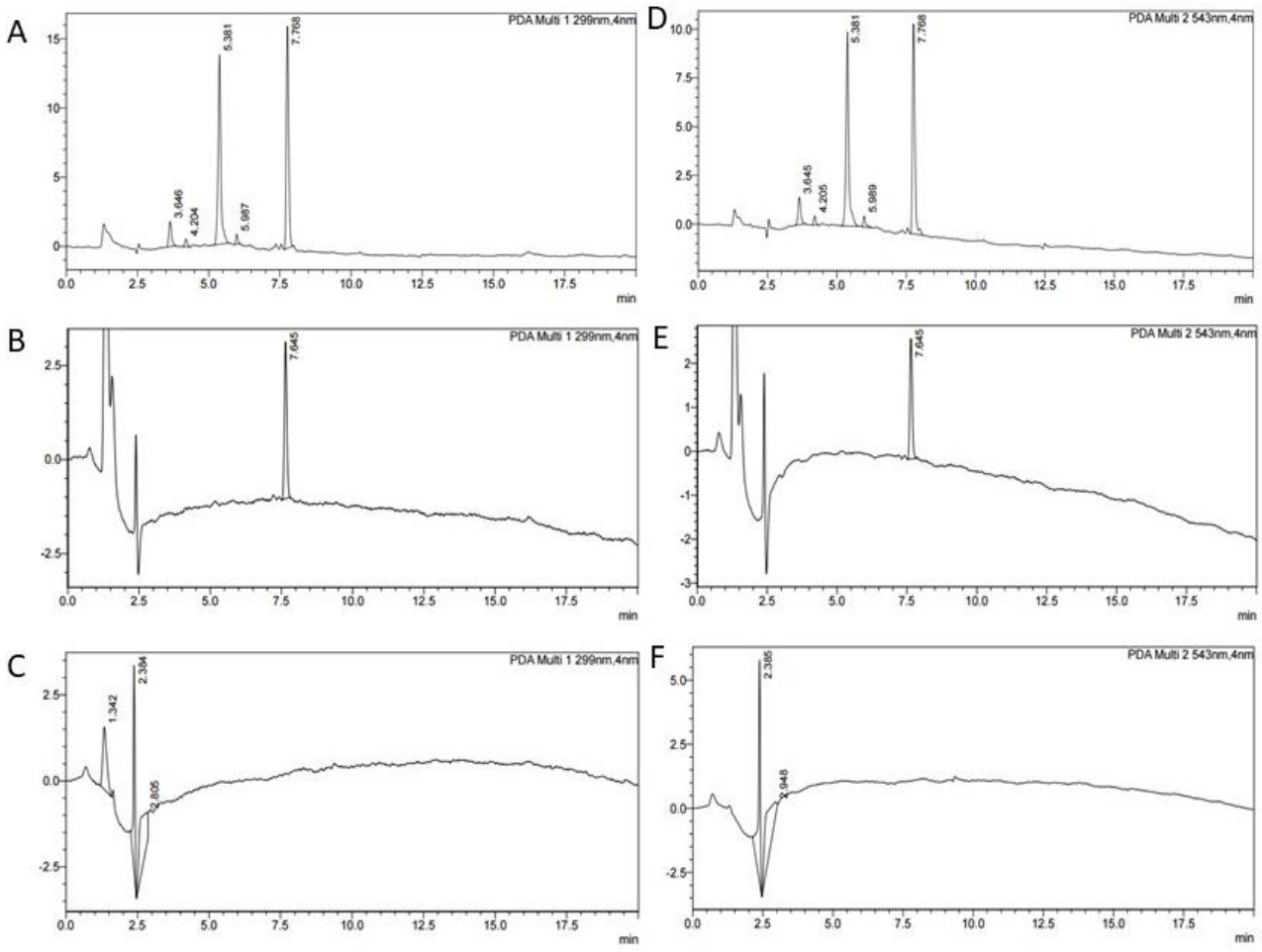

Fig. 6 Graph depicting HPLC chromatogram at 299nm and 543nm for SR dye A) and D) Input, B) and E) MBBR output, C) and F) UV/Fenton output.

Table 2 : Quantitative peak reduction area from HPLC chromatogram at 299nm and 543nm.

	Area of peaks at 299nm		
Sample Name	RT 3.6	RT 5.3	RT 7.7
Input	12043	92371	91519
Mbbr Output	0	2147	23108
AOP	0	0	0
	Area of peaks at 543nm		
	RT 3.6	RT 5.3	RT 7.7
Input	9577	68223	64517
Mbbr Output	0	1888	14691
AOP	0	0	0

HPLC was used to confirm the degradation of SR dye after each stage, that is, Input, MBBR Output, and UV/Fenton for 299nm and 543nm. The method was developed for both dyes. Fig. S7 shows the r^2 value obtained upon standardization. Chromatogram for the Input sample of SR dye, given in Fig. 6A and Fig. 6D, both display several distinct peaks, with major retention times at approximately 3.6, 5.3, and 7.7 min, corresponding to the parent dye and its primary constituents. Following treatment with the MBBR, the chromatogram Fig. 6B and Fig. 6E reveals substantial changes in the primary dye peaks at RT 3.6, 5.3, and 7.7 min, which can also be observed from the reduction in peak area mentioned in Table 2. This change indicates

that the MBBR process has effectively degraded the parent dye compound, likely producing intermediate metabolites or transformation products, as evidenced by the appearance of new chromatographic signals and reduction in peak intensity for the original dye. Further treatment with the UV/Fenton process Fig. 6C and Fig. 6F results in the near absence of the initial dye peaks. The reduction of the original dye peaks and the generation of new chromatographic signals demonstrate that AOP achieves an even higher degree of dye degradation.

3.6. PILOT-SCALE OPERATION OF THE MBBR – UV/FENTON TREATMENT SYSTEM

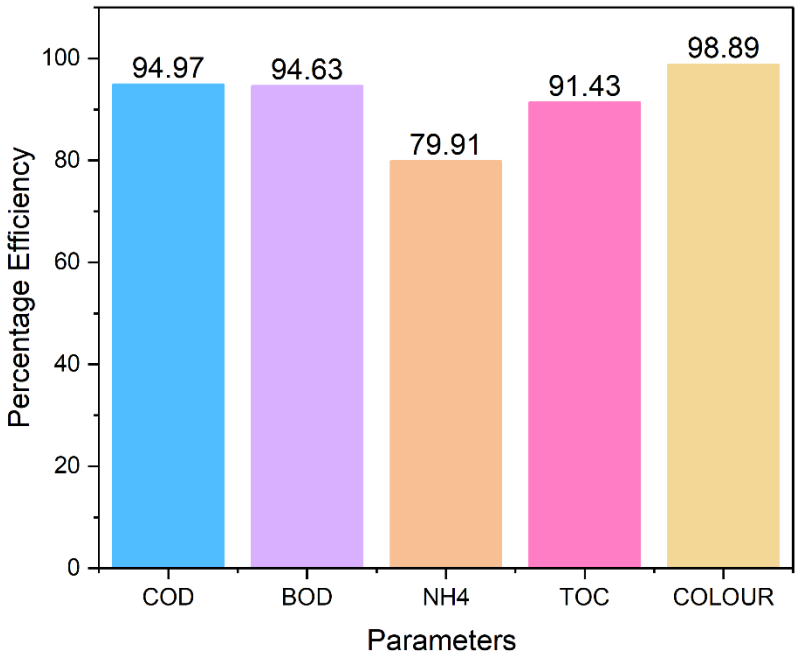

Fig 7. Graph illustrating reduction efficiencies of parameters for 1000L/d MBBR—UV/Fenton system.

Table 3: Characteristics of dye wastewater after each stage of treatment for 1000L/d MBBR—UV/Fenton system**.**

Parameters	Input	MO	UV/Fenton
COD mg/l	585 ± 57.4	83.8 ± 41.5	29.4 ± 24.7
BOD mg/l	199.5 ± 60.4	24.5 ± 8	10.7 ± 1.7
pH	7.22 ± 0.17	7.25 ± 0.31	7.32 ± 0.14
Absorbance	1.8 ± 0.5	1.1 ± 0.4	0.03 ± 0.02
TOC mg/l	173.2 ± 41.4	40.5 ± 7.3	14.8 ± 9.3
Nh_4-N mg/l	57.3 ± 7.8	15.5 ± 9.1	11.5 ± 3.2

As shown in Fig. 7 and Table 3, the integrated MBBR-UV/Fenton system performed better. The Organic loading rate for the system was 585g COD/d, and the dissolved oxygen of the MBBR reactor was 3mg/l. The system achieved consistent removal efficiencies of 94.97% for COD and 94.63% for BOD, indicating highly effective degradation of dye wastewater. TOC removal was 91.43%, confirming substantial mineralization of organic compounds. NH_4-N removal efficiency was 79.91%. Most notably, the system showed an absorbance reduction of 98.89%, demonstrating the exceptional performance of the MBBR-UV/Fenton at color removal. The MBBR successfully decreased bulk organic load and showed that the combined MBBR-UV/Fenton system is very successful in treating wastewater containing textile dyes, starting dye breakdown, following which UV/Fenton achieved near-complete removal of leftover color. As per the standards prescribed by the Indian Central Pollution Control Board, the standards are BOD ≤ 30 mg/L, COD ≤ 50 mg/L, TOC 20 mg/l and ammoniacal nitrogen (as N) ≤ 15 mg/L. The treated effluent exhibited COD 29.4 ± 24.7 mg/L, BOD 10.7 ± 1.7 mg/L, Absorbance 0.03 ± 0.02 , TOC 14.8 ± 9.3 mg/L and NH_4–N 11.5 ± 3.2 mg/L, which are all below the corresponding CPCB limits. These findings produce effluent quality appropriate for release or possible reuse.

HPLC analysis was conducted to evaluate the molecular degradation of SR dye through sequential MBBR-UV/Fenton treatment at detection wavelengths of 299 nm and 543 nm. The untreated dye samples, Fig. S8A and Fig. S8D, displayed multiple peaks of the parent dye. Peak RT observed was at 4.2, 5.3, and 11.2 min for the Input, with similar patterns were

observed for 543nm. Following MBBR treatment, Fig. S8B and Fig. S8E, significant peak intensity reduction occurred, indicating partial biodegradation and formation of intermediate metabolites. Residual compounds were detected at modified retention times, demonstrating enzymatic transformation of the parent dye structure. Subsequent UV/Fenton treatment Fig. S8C and Fig. S8F resulted in near-complete elimination of original dye peaks. Only trace compounds remained with dramatically reduced intensities, while signals at 543 nm virtually disappeared, confirming extensive decolorization and chromophore destruction.

Both treatment cycles demonstrated consistent degradation patterns, validating the reproducibility and effectiveness of the integrated MBBR-UV/Fenton system. The progressive simplification of chromatographic profiles provides molecular-level evidence of successful SR dye degradation through the sequential biological-chemical oxidation process.

3.7. ECONOMIC ANALYSIS

Table 4: Capex of MBBR- UV/Fenton method for 1000L.

Sr. NO	Item name	Quantity	Price	Final Price
1	Air Blower	2	$ 150.69	$ 301.37
2	1000L IBC tank	3	$ 69.55	$ 208.64
3	Disc Diffuser	4	$ 13.91	$ 55.64
4	UV Lamp	1	$ 57.11	$ 57.11
5	Bio-carrier	1	$ 92.73	$ 92.73
6	Kirloskar 0.5hp pump	1	$ 34.72	$ 34.72
7	Miscellaneous Expense (Maintenance and Sludge handling)	1	$ 115.91	$ 115.91
			Total	$ 866.12

***The price is mentioned as per the year 2025**

Sr. No.	Chemical name	Pack size	Price per pack	Quantity used	Calculated Price
1	Hydrogen Peroxide	500 ml	$ 7.81	230 ml	$ 3.60
2	Ferrous Sulphate Heptahydrate	500 g	$ 2.03	100g	$ 0.41
3	Conc. Sulfuric Acid	500 ml	$ 2.89	54 ml	$ 0.29
4	Sodium Hydroxide	500 gm	$ 2.64	50 g	$ 0.26
				Total	$ 4.56

Table 5: OPEX of MBBR- UV/Fenton method for 1000L.

The economic analysis affirms the viability of the integrated MBBR–UV/Fenton system for industrial dye wastewater treatment within the Indian market context. The total capital cost (CAPEX) displayed in Table 4 is $866.12 per m³ and encompasses essential equipment, including air blowers, IBC tanks, bio-carriers, pumps, diffusers, and automation components. These figures are comparable to previously reported MBBR-based installations, where CAPEX typically ranges from $700 to $1,200 per m³ depending on treatment scale and configuration (Nagel-Hassemer *et al.* 2011, Khatri *et al.* 2018).

Operational costs (OPEX) displayed in Table 5 are primarily driven by chemical requirements, with hydrogen peroxide as the largest contributor, followed by iron catalyst, alkali, and acid for pH adjustment, resulting in a total chemical cost of $4.56 per m³. Electricity input accounts for $0.27 per m³, leading to an overall OPEX of $4.83 per m³. This is consistent with findings

from comparable hybrid biological-advanced oxidation systems, where OPEX typically falls between $3.50 and $6.50 per m³ in the Indian context.

Distributing CAPEX over the projected lifespan reduces its impact per volume treated, making OPEX a critical determinant of economic sustainability, especially with increasing throughput. Prior research highlights that optimized process parameters and chemical dosing can further reduce recurring costs by up to 20% (Kallawar and Bhanvase 2024). Overall, the hybrid system offers robust dye removal at competitive costs, supporting its application for the treatment of industrial dye effluent management.

4. CONCLUSION

This study successfully demonstrated the synergistic potential of an integrated MBBR-UV/Fenton system for dye wastewater treatment, achieving better performance over conventional approaches. This system effectively combines the biological capabilities of biofilm-mediated processes with chemical oxidation, resulting in superior pollutant removal efficiency. Key findings reveal that the optimized MBBR-UV/Fenton system reduced color by 98.37%, COD by 84.18%, BOD_5 by 98.67%, and NH_4-N by 74.46% for SR dye. Furthermore, similar results were observed when the system was scaled up to 1000 L/d of 100 ppm of SR, wherein the system reduced color by 98.89%, COD by 94.97%, BOD_5 by 94.63%, and NH_4-N by 79.91%. The CAPEX of the system was $866.12 per m³, and the OPEX of the system was found to be $4.83 per m³.

Future research should focus on process upgradation through carrier materials with improved biofilm properties, monitoring of residual Fe, residual H_2O_2, and iron sludge generation to more comprehensively evaluate the environmental safety, operational feasibility, and scalability of the treatment process. and AI-driven control systems for real-time optimization. Integration with emerging technologies such as membrane bioreactors could further enhance removal efficiency, while energy optimization studies incorporating renewable energy sources would promote sustainable operation. Resource recovery potential, including biogas generation and nutrient recovery, presents opportunities for circular economy implementation. Pilot-scale validation with real industrial wastewater containing diverse pollutants and long-term operational studies is essential for assessing system durability and performance consistency. Additionally, treatment of micropollutants and integration with Industry frameworks would advance smart manufacturing applications. The successful MBBR-UV/Fenton demonstration establishes a robust foundation for sustainable dye wastewater treatment with significant potential for addressing global water pollution challenges while promoting circular economy principles in the industry.

5. ACKNOWLEDGEMENT

S. Prabhudesai sincerely acknowledges BITS Pilani K. K. Birla Goa Campus for the Fellowship. The authors acknowledge CDRF Grant Reference: C1/23/119 for providing research funding. The authors deeply acknowledge the Center for Sophisticated Instruments Facility (CSIF)-BITS Pilani K.K. Birla Campus, Goa, India, for FE-SEM. The author acknowledges the Department of Chemistry (BITS Pilani K. K. Birla Goa Campus) for HPLC analysis. The author also acknowledges Ms. Shobha Mule from the Department of Chemistry (BITS Pilani K. K. Birla Goa Campus) for her assistance in HPLC method development and analysis.

Author Contributions: S. Prabhudesai: Conceptualization, Methodology, Investigation, Validation, Formal analysis, Software, Visualization, Writing-Original draft preparation. Prof. S. Mutnuri: Writing-Review, Project administration, Supervision, Funding acquisition.

6. REFERENCES

Afanga, H., Zazou, H., Titchou, F.E., Rakhila, Y., Akbour, R.A., Elmchaouri, A., Ghanbaja, J. and Hamdani, M., 2020. Integrated electrochemical processes for textile industry wastewater treatment: System performances and sludge settling characteristics. *Sustainable Environment Research*, 30(1), pp. 1–11. https://doi.org/10.1186/s42834-019-0043-2.

Agustina, T.E., Teguh, D., Rismawati, R. and Patika, Y.,2019. Study on Fenton reaction for degradation of procion red synthetic dyes. *AIP Conference Proceedings*, 2085. https://doi.org/10.1063/1.5095046.

Chandrika, K.C., Prabhu, T.N., Kiran, R.R.S. and Krishna, R.H., 2022. Applications of artificial neural network and Box-Behnken Design for modelling malachite green dye degradation from textile effluents using TiO 2 photocatalyst. *Environmental Engineering Research* , 27(1): 200553. https://doi.org/10.4491/eer.2020.553.

Francis, A. and Sosamony, K.J., 2016. Treatment of Pre-treated Textile Wastewater using Moving Bed Bio-film Reactor. *Procedia Technology*, 24, pp. 248–255. https://doi.org/10.1016/j.protcy.2016.05.033.

Gzar, H.A., Al-Rekabi, W.S. and Shuhaieb, Z.K., 2021. Applicaion of Moving Bed Biofilm Reactor (MBBR) for Treatment of Industrial Wastewater: A mini Review. *Journal of Physics: Conference Series*, 1973(1). https://doi.org/10.1088/1742-6596/1973/1/012024.

Haddad, M. El, Regti, A., Laamari, M.R., Mamouni, R. and Saffaj, N., 2014. Use of Fenton reagent as advanced oxidative process for removing textile dyes from aqueous solutions. *J. Mater. Environ. Sci.* pp. 667-674.

Hu, X., Wang, X., Ban, Y. and Ren, B., 2011. A comparative study of UV-Fenton, UV-H2O2 and Fenton reaction treatment of landfill leachate. *Environmental Technology*, 32(9), pp. 945–951. https://doi.org/10.1080/09593330.2010.521953.

Kallawar, G.A. and Bhanvase, B.A., 2024. A review on existing and emerging approaches for textile wastewater treatments: challenges and future perspectives. *Environmental science and pollution research international*, 31(2), pp. 1748–1789. https://doi.org/10.1007/s11356-023-31175-3.

Khanageltri, J., Nidheesh, P. V., Anantha Singh, T.S. and Suresh Kumar, M., 2018. Advanced oxidation processes based on zero-valent aluminium for treating textile wastewater. *Chemical Engineering Journal*, 348. pp. 67–73. https://doi.org/10.1016/j.cej.2018.04.074.

Lucas, M.S. and Peres, J.A., 2006. Decolorization of the azo dye Reactive Black 5 by Fenton and photo-Fenton oxidation. *Dyes and Pigments*, 71(3), pp. 236–244. https://doi.org/10.1016/j.dyepig.2005.07.007.

Nagel-Hassemer, M.E., Carvalho-Pinto, C.R.S., Matias, W.G. and Lapolli, F.R., 2011. Removal of coloured compounds from textile industry effluents by UV/H 2O2 advanced oxidation and toxicity evaluation. *Environmental Technology*, 32(16), pp. 1867–1874. https://doi.org/10.1080/09593330.2011.566893.

Papić, S., Vujević, D., Koprivanac, N. and Šinko, D., 2009. Decolourization and mineralization of commercial reactive dyes by using homogeneous and heterogeneous Fenton and UV/Fenton processes. *Journal of Hazardous Materials*, 164(2–3), pp. 1137–1145. https://doi.org/10.1016/j.jhazmat.2008.09.008.

Park, H.O., Oh, S., Bade, R. and Shin, W.S., 2010. Application of A2O moving-bed biofilm reactors for textile dyeing wastewater treatment. *Korean Journal of Chemical Engineering*, 27(3), pp. 893–899. https://doi.org/10.1007/s11814-010-0143-5.

Phanwilai, S., Kangwannarakul, N., Noophan, P. (Lek), Kasahara, T., Terada, A., Munakata-Marr, J. and Figueroa, L.A., 2020. Nitrogen removal efficiencies and microbial communities in full-scale IFAS and MBBR municipal wastewater treatment plants at high COD:N ratio. *Frontiers of Environmental Science and Engineering*, 14(6), pp. 1–13. https://doi.org/10.1007/s11783-020-1374-2.

PIECZYKOLAN, B., PŁONKA, I. and BARBUSIŃSKI, K., 2016. Discoloration of Dye Wastewater By Modified Uv-Fenton

Process With Sodium Percarbonate. *Architecture, Civil Engineering, Environment*, 9(4), pp. 135–140. https://doi.org/10.21307/acee-2016-060.

Rusten, B., Eikebrokk, B., Ulgenes, Y. and Lygren, E., 2006. Design and operations of the Kaldnes moving bed biofilm reactors. *Aquacultural Engineering*, 34(3), pp. 322–331. https://doi.org/10.1016/j.aquaeng.2005.04.002.

Samawi, M.F., Taba, P. and Lanuru, M., 2025. Optimizing Community Health Center Effluent Treatment with Moving Bed Biofilm Reactor Technology Combined with Activated Carbon and Chlorine. *Nature Environment and Pollution Technology*, *24*(1), pp.1-12. https://doi.org/10.46488/NEPT.2025.v24i01.D1700

Tabaraki, R., Zadkhast, S., Najafi, A. and Rezaei, V., 2023. Performance and cost analysis of dye wastewater treatment by Fenton , electro - Fenton , and biosorption : Box - Behnken experimental design and response surface methodology. *Biomass Conversion and Biorefinery*, 13(15), pp. 13527–13537. https://doi.org/10.1007/s13399-022-02809-2.

Tuncer, N. and Sönmez, G., 2023. Removal of COD and Color from Textile Wastewater by the Fenton and UV/H2O2 Oxidation Processes and Optimization. *Water, Air, and Soil Pollution*, 234(2). https://doi.org/10.1007/s11270-023-06095-0.

Wang, X., Chen, S., Bi, X., Chen, N., Yang, T., Wang, L., Maletskyi, Z. and Ratnaweera, H., 2023. Morphological image analysis of biofilm evolution with quantitative analysis in a moving bed biofilm reactor. *Science of the Total Environment*, p. 159-199. https://doi.org/10.1016/j.scitotenv.2022.159199.

Yang, X. and López-Grimau, V., 2021. Reduction of cost and environmental impact in the treatment of textile wastewater using a combined mbbr-mbr system. *Membranes*, 11(11). https://doi.org/10.3390/membranes11110892.

7. BACKGROUND INFORMATION FOR RECORD (NOT TO BE PRINTED)

Conflicts of Interest: The authors declare that they have no personal relationship or financial interest that could have influenced the reported work in this publication.